Desalination and Water Treatment
www.deswater.com

doi: 10.5004/dwt.2020.25437

185 (2020) 262–276
May

Modeling and optimization of removal of strontium and cesium from aqueous streams by size enhanced ultrafiltration using chitosan derivative

Edward Kavitha*, Mukund Dalmia, Alexander Mammen Samuel, Sivaraman Prabhakar, Mathur P. Rajesh

Department of Chemical Engineering, SRM Institute of Science and Technology, Kattankulathur, Chennai, Tamilnadu, India, 603203, Tel. +91-9445609098; email: kavi0910@gmail.com (E. Kavitha), Tel. +91-9840501588; email: mukunddalmia148@gmail.com (M. Dalmia), Tel. +91-9869346720; email: alexandermsamuel@gmail.com (A.M. Samuel), Tel. +91-9445259977; email: sivaprabha50@gmail.com (S. Prabhakar), Tel. +91-9677149224; email: mprajesh@gmail.com (M.P. Rajesh)

Received 27 July 2019; Accepted 4 January 2020

ABSTRACT

Treatment of fission product aqueous waste is a challenging problem as their chemical concentrations are too low but have significant radiation hazard due to their half-life. The current methods of co-precipitation lead to more sludge and require more space for confinement. Size enhanced ultrafiltration (SEUF) is an emerging technology with a potential not only to effectively separate the species of interest namely Strontium [Sr(II)] and Cesium [Cs(I)] but also recover them by reversing certain chemical conditions. The present paper concerns the removal of Sr(II) and Cs(I) from aqueous streams using SEUF. The studies were conducted using chitosan derivative, carboxymethyl chitosan (CMCh) as a size enhancing agent. The effect of process variables such as initial pH, loading ratio (P/M), and initial concentration of Sr(II) and Cs(I) on the percentage rejection and binding capacity have been studied. The design of experiments was performed by response surface methodology (RSM). The maximum percentage rejection of Cs(I) was found to be 99% at the following optimum process conditions: initial pH of the feed solution is 12, initial concentration of Cs(I) is 10 mg/L, and P/M value is 0.5. The maximum percentage rejection of Sr(II) was found to be 99% at the following optimum process conditions: initial pH of the feed solution is 12, initial concentration of Sr(II) is 9 mg/L, and P/M value is 0.5. The results show that SEUF with CMCh could be an effective method for the removal of Sr(II) and Cs(I).

Keywords: Ultrafiltration; Heavy metals; Strontium; Cesium; Radio-active species; Chitosan

1. Introduction

Water has become a scarce, valuable commodity due to the increased population, living style of people, industrial growth, and technological development. Water resources have been polluted by an enormous volume of industrial effluents containing organic, inorganic, biological, and toxic pollutants. Effluents from industries such as electroplating, mining, textile, tannery, dyes, pigments, and nuclear power plants have been identified to contain a high level of heavy metals [1–3]. Among the toxic contaminants, the radio-active wastes are considered to be more dangerous as it contains isotopes with very long half-life period. ^{90}Sr and ^{137}Cs are the two chief isotopes formed during the nuclear fission process, and most of the low-level nuclear wastes contain these two fission products [4,5]. The half-life of all the strontium nuclides is <65 d, except ^{90}Sr, which has a half-life of 29 y [6,7]. The chemical form of Strontium strongly influences its environmental transport, and it can move down through soil with percolating water to groundwater. They have direct effects on humans and animals and can seriously affect human health and the environment. The principal source of internally deposited strontium is the gastrointestinal absorption from food or water. The primary health issues related to strontium

* Corresponding author.

are bone tumors and tumors of blood cell forming organs [5]. Cesium is naturally present as the isotope ^{133}Cs. Breakdown of Uranium in fuel elements can produce two radio-active forms of cesium, ^{134}Cs, and ^{137}Cs. The half-life period of ^{134}Cs is 2 y. ^{137}Cs is a toxic radionuclide with the long half-life of 30 y, high solubility, and higher activity [8].

^{137}Cs and ^{90}Sr are the two species present in low-level radioactive waste in nuclear power plants [4,5]. Even though, the chemical concentration of strontium and cesium isotopes are abysmally low (<<ppb), the radio-toxicity is quite worrisome. These are long-lived isotopes, and the philosophy of waste treatment is to reduce the volume of the waste and confine them in a desolate environment under surveillance for an extended period. Conventional treatment methods such as adsorption [9–13], chemical precipitation [14–17], ion exchange [18–20], and biological treatment [21–23] have been employed for the separation of Sr(II) and Cs(I) from wastewater. The process of separating them from aqueous wastes is by co-precipitation of strontium as phosphate along with calcium phosphate [24], while Cs is separated along with copper-ferro-cyanide precipitate through ion exchange mechanism and also by flocculation [25,26]. However, chemical precipitation processes have a low decontamination factor [27]. Also, the chemical precipitation process may not form an insoluble precipitate of radioactive wastes which is present in the lower concentration [28]. At deficient levels, ion exchangers were also used. In all these cases, it involves the addition of a huge volume of chemicals which in-turn leads to the generation of large volumes of sludge and the removal efficiency is also quite low. The separation of Cs(I) and Sr(II) by sorption has been proved to be an efficient process with a high decontamination factor [13]. However, these processes have some limitations such as limited selectivity, poor regeneration, and reusability of adsorbent or ion exchange resin [28]. Also, these processes have limitations such as equilibrium governed processes, usually requiring long operating time, may require additional treatment for the recovery, sludge disposal, and large footprint area.

For the removal of these trace contaminants from aqueous streams, membrane separation processes such as reverse osmosis (RO) and nano-filtration (NF) have been used [29–31]. Because of the inherent limitations of high-pressure operation and limited volume reduction of contaminated streams, they could not, however, be adopted on a large scale [30]. In recent years, there is a growing interest in the application of ultrafiltration based membrane separation processes for the removal of radio-active contaminants from wastewater. Size enhanced ultrafiltration (SEUF) is an emerging separation process, which involves the addition of water-soluble polymer with the metal ions to be removed and separation by UF. In this process, Sr(II) and Cs(I) to be separated from aqueous streams, complex with polymer ligands to form a macromolecular structure which can be easily retained by UF membrane. This process has been employed for the following reasons: (i) all the functional groups in the ligands can be utilized, (ii) the contact duration required is relatively less, (iii) large volume can be treated within a short span of time, (iv) volume reduction, and (vi) less sludge formation [32].

In this work, chitosan derivative carboxymethyl chitosan (CMCh) has been utilized for the removal of Sr(II) and Cs(I) as a size enhancing agent. The coordination mechanism of Sr(II) and Cs(I) with CMCh is utilized for the separation of it. Chitosan is a cheap, biodegradable, and abundantly available polymer. It has hydroxyl and amino groups in its structure. It can be modified physically and chemically to incorporate new and desired functional groups to complex with the metal ions. Some of the derivatives of chitosan such as pyridyl methyl chitosan [33], amino acid conjugated chitosan [34], dithiocarbamate chitosan [35], crown ether cross-linked chitosan [36], EDTA linked chitosan [37], polyethylenimine cross-linked chitosan [38], and CMCh [39,40] have been reported in the literature. The removal of metal ions using chitosan derivatives by SEUF has been reported in only a few papers. In this paper, the separation of Sr(II) and Cs(I) using water-soluble CMCh have been investigated with SEUF under various experimental conditions such initial pH of the feed solution, P/M, and initial concentration of Sr(II) and Cs(I) in feed solution in detail. Scanning electron microscope (SEM), energy-dispersive X-ray analysis (EDX), and Fourier transform infrared spectroscopy (FTIR) analysis were used to characterize the complex of Sr(II)-CMCh and Cs(I)-CMCh.

The design of experiments (DoE) has been performed using response surface methodology (RSM) combined with a face-centered central design. RSM is a set of mathematical and statistical tools used for the DoE, and for improving and optimizing the processes [41]. This method can be utilized for evaluating the effects of individual process variables and their relative significance, the interactive effects amongst the process variables and also for assessing the optimum process conditions for desired process responses [42]. RSM generally involves the following steps: the selection of process variables, DoE, and formulation of a suitable model for the experimental data to analyze the process variables and their significant interaction upon process responses, and the optimization of process conditions [43]. The analysis of variance (ANOVA) was performed to evaluate the significance of the model, process variables, and their interactive effects on the process responses and also to validate the model equations. The process responses such as percentage rejection of Sr(II) and Cs(I), and binding capacity of CMCh with Sr(II) and Cs(I) have been investigated, and the optimization studies were performed to maximize the process responses.

2. Materials and methods

2.1. Materials

The stock solutions of Sr(II) and Cs(I) of concentration 100 mg/L were prepared by $Sr(NO_3)_2$ and $CsNO_3$, (AR grade), respectively. The pH of the aqueous solutions was adjusted using a dilute solution of NaOH (0.1 M) and HCl (0.1 M). All the chemicals used were of analytical grade. The commercially available water-soluble CMCh (M/s. Everest Biotech, Banglore) was used.

2.2. Experimental setup

Cylindrically coated domestic polyethersulfone (PES) UF membrane element (M/s Rupali Industries, Mumbai) of molecular weight cut-off (MWCO) 50 kDa was used for the studies. The UF candle consists of PES coated on a cylindrical surface with a diameter 0.054 m, length of 0.27 m, and a membrane area of 0.05 m^2. The flow of feed was from the outside surface of the membrane to the inner side of the

membrane. PES UF membranes on the industrial scale are considered to be the most economical and feasible for the treatment of heavy metal contaminants. PES membrane is more flexible, and it has exceptional chemical, electrical, mechanical, and thermal properties such as exceptional heat-aging resistance and environmental endurance as well as easy processing [44,45]. The ultrafiltration membrane of MWCO 50 kDa is the readily available commercial membrane. This 50 kDa PES membrane was chosen owing to its higher rejection capacity and moderate permeate flux. The studies have been carried out in the dead-end mode operation. In dead-end mode, the total volume of the feed passes through the membrane, leaving all the components that are larger than the pores of the membrane, in or on the membrane surface. Unlike cross-flow systems, it does not require more energy. Fig. 1 shows the schematic diagram of the experimental setup.

2.3. Experimental procedure for the removal of Sr(II) and Cs(I) by SEUF

Aqueous feed solutions of Sr(II) and Cs(I) were prepared with the initial concentrations in the range of 2–10 mg/L. The size enhancing polymer CMCh was added with the feed solution in the range of loading ratio (P/M) 0.5–3, and the initial pH of the feed solution was adjusted from 2 to 12. The feed solution was supplied to the membrane through a pump operated at a pressure of 2 bar and a flowrate of 10 LPH. The feed solution was passed through the outer surface of the membrane. The permeate coming out from the interior surface of the membrane was collected. After completion of the filtration process, the retentate held inside the candle was also collected. Both the samples were analyzed with atomic absorption spectroscopy to evaluate the concentration of Cs(I) and Sr(II).

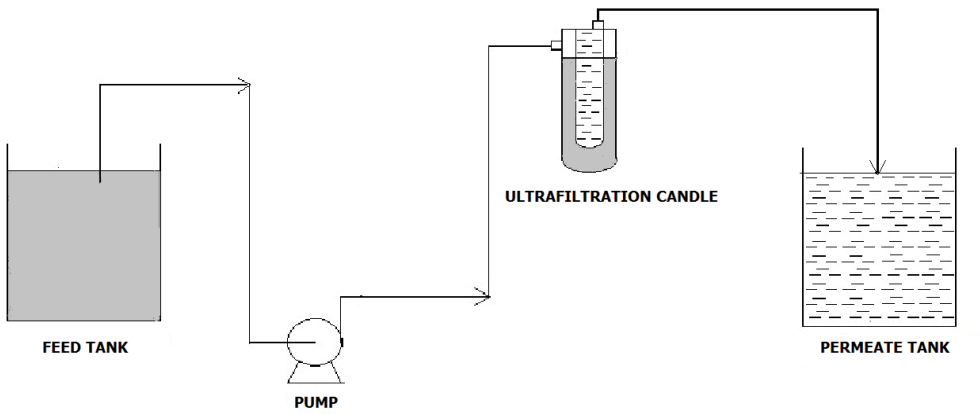

(a)

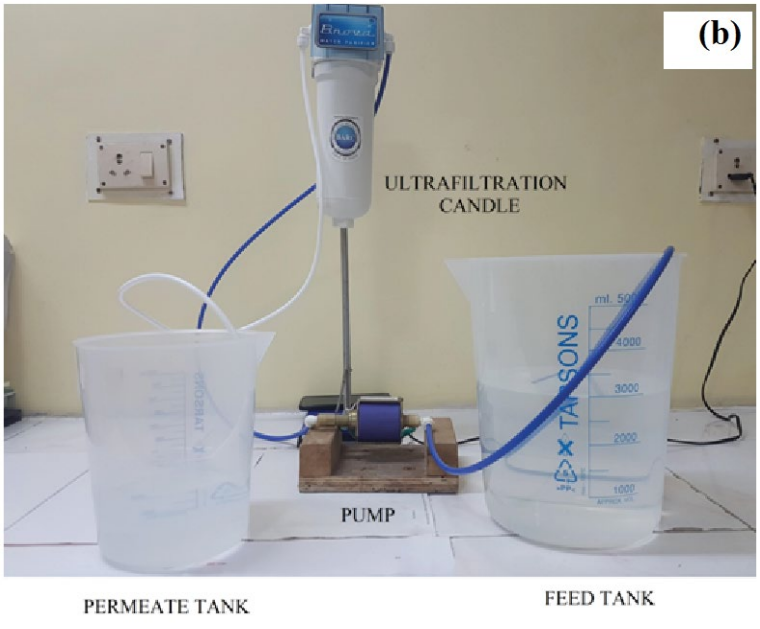

Fig. 1. (a) Schematic diagram of experimental setup and (b) experimental setup. Feed: 5 L, flowrate: 10 LPH, and operating pressure: 2 bar.

The percentage rejection R, which measures the separation capability of membrane, was calculated using Eq. (1).

$$R = \left(1 - \frac{C_p}{C_f}\right) \times 100(\%) \quad (1)$$

where C_f and C_p are the concentration of a metal ion in feed and permeate, respectively (mg/L).

The binding capacity of a polymer, which indicates the quantity of metal ion uptake, was calculated using Eq. (2) [46].

$$q = \left(\frac{C_f - C_p}{a \times 1{,}000}\right) V \quad (2)$$

where q is the binding capacity (mg/g), a is the mass of polymer used (g), and V is the volume of feed solution (mL).

2.4. Experimental design and optimization of conditions using RSM

Literature shows the successive results for the precise prediction and optimization of process variables using RSM for the removal of Cu(II), Ni(II), Co(II), Zn(II), and Cr(VI) [46,47]. The central composite design (CCD) was widely used for obtaining response surface models to get the relation between process input variables and process responses since it does not require excessive experimental runs [46–48]. In this work, RSM has been adopted for the studies on the separation of Cs(I) and Sr(II) from aqueous streams. The total number of experimental runs (N) required can be calculated by using the following Eq. (3):

$$N = 2^n + 2n + N_0 \quad (3)$$

where n represents the number of factors analyzed and N_0 represents the number of center points.

Optimization was carried out using the statistical software Design Expert 10.0.0 (Stat-Ease, Inc., Minneapolis, MN, USA). In this study, face-centered CCD (Tables 1 and 2) was used to (i) design the experiments, (ii) analyze the input variables and interactive effect of input variables on process responses, (iii) predict the mathematical model equations, and (iv) obtain the optimized parameters for the removal of Sr(II) and Cs(I). In this study, the following input variables were selected: (i) initial concentration of the feed, (ii) initial pH of the feed solution, and (iii) polymer to metal ratio (loading ratio), P/M [40,46]. The following responses were obtained from the experimental runs performed based on the DoE: (i) percentage rejection of Sr(II) and Cs(I) using CMCh and (ii) binding capacity of CMCh with Sr(II) and Cs(I) [40,49].

Response surface models are widely used to approximate the experimental data using polynomial expressions. Response surface model is given by the Eq. (4):

$$y(x) = f(x) + \varepsilon \quad (4)$$

Table 1
Design of experiments for the removal of Sr(II) using CMCh

Std.	Run	Factor 1	Factor 2	Factor 3	Response 1	Response 2
		A: initial pH	*B*: P/M (w/w)	*C*: initial concentration (mg/L)	Percentage rejection (%)	Binding capacity (mg/g)
1	9	2	0.5	2	3.25	65
2	10	12	0.5	2	35.25	705
3	18	2	3	2	8.5	28.33
4	14	12	3	2	68.6	228.67
5	12	2	0.5	10	10.24	204.8
6	3	12	0.5	10	99.1	1,982
7	19	2	3	10	10.5	35
8	8	12	3	10	99.6	332
9	1	2	2	6	21.97	109.85
10	17	12	2	6	74.6	373
11	11	7	0.5	6	53	1,060
12	13	7	3	6	69.15	230.5
13	5	7	2	2	4.1	20.5
14	4	7	2	10	3.8	19
15	16	7	2	6	64.6	323
16	2	7	2	6	64.6	323
17	15	7	2	6	64.6	323
18	7	7	2	6	64.6	323
19	20	7	2	6	64.6	323
20	6	7	2	6	64.6	323

Table 2
Design of experiments for the removal of Cs(I) using CMCh

Std	Run	Factor 1	Factor 2	Factor 3	Response 1	Response 2
		A: initial pH	*B*: P/M (w/w)	*C*: initial concentration (mg/L)	Percentage rejection (%)	Binding capacity (mg/g)
1	15	2	0.5	2	85.6	1,712
2	18	12	0.5	2	95.7	1,914
3	11	2	3	2	90.72	302.4
4	20	12	3	2	97.5	325
5	4	2	0.5	10	98.24	1,964.8
6	14	12	0.5	10	98.5	1,970
7	3	2	3	10	98.32	327.73
8	16	12	3	10	99.04	330.13
9	5	2	2	6	91.57	457.85
10	8	12	2	6	98.32	491.6
11	19	7	0.5	6	91.56	1,831.2
12	7	7	3	6	95	316.67
13	17	7	2	2	90.9	454.5
14	1	7	2	10	98.2	491
15	2	7	2	6	93.5	467.5
16	9	7	2	6	93.5	467.5
17	12	7	2	6	93.5	467.5
18	10	7	2	6	93.5	467.5
19	13	7	2	6	93.5	467.5
20	6	7	2	6	93.5	467.5

where $y(x)$ represents the unknown function of interest, $f(x)$ represents the known polynomial function of × and ε is the random error.

A second-order polynomial model equation can be developed to fit the experimental data obtained from the experimental runs performed based on DoE. The model Eq. (5) is given by the following relationship:

$$\hat{Y} = b_0 + \sum_{i=1}^{k} b_i x_i + \sum_{i=1}^{k} b_{ii} x_i^2 + \sum_{i=1}^{k} \sum_{j=1}^{j \le i} b_{ij} x_i x_j \quad (5)$$

where $\hat{Y}$ represents the predicted response (predicted percentage rejection, binding capacity). x_i represents the coded levels of the process input variables. b_0, b_i, b_{ii}, and b_{ij} are the regression coefficients determined through the least square regression (offset term, main, quadratic, and interaction effects). Least square regression determines the partial derivatives of the coefficients and minimizes the sum of the squares of the residuals of the predicted response values from the actual values.

The basic form of least square regression is given by the following Eq. (6) [50]:

$$b = \left[x'x\right]^{-1} x'y \quad (6)$$

where x represents (N × L) the extended design matrix of the coded levels of the process input variables, x' represents its transpose, and y (N = 1) represents column vector found experimentally, that contains the values of the response at each sample point. The number of experimental runs is represented by N, and the number of regression coefficients within the extended response surface model is represented by L [49].

3. Results and discussions

3.1. Characterization of CMCh, CMCh-Cs(I) complex, and CMCh-Sr(II) complex with SEM, EDX, and FTIR

The surface morphology and elemental composition of CMCh, Complex of CMCh with Cs(I) and Sr(II) were analyzed by SEM, EDX, and FTIR as shown in Figs. 2, 3. The SEM image of CMCh shows its amorphous and porous nature (Fig. 2a). The surface morphology was modified after complexation with Cs(I) as shown in Fig. 2b. The change in the surface morphology was also observed after complexation with Sr(II) as shown in Fig. 2c. The EDX analysis as shown in Fig. 3b also reveals the confirmation of the complexation of CMCh with Cs(I) as it provides the peaks C, O, and N corresponding to CMCh and the peaks corresponding to Cs(I). The peaks corresponding to CMCh and Sr(II) confirm the complexation of CMCh with Sr(II) as shown in Fig. 3c.

The FTIR spectra of CMCh, Cs(I) with CMCh complex, and Sr(II) with CMCh complex are shown in Fig. 4. Fig. 4a shows the FTIR spectrum of CMCh. The peak at 1,521 cm^{-1} corresponds to C=C, C=N stretch. The peak at 1,213 cm^{-1} represents the C–O stretch and the peak at 1,150 cm^{-1} reflects the C–O stretch. The peak at 1,622 cm^{-1} corresponds to carboxyl group and $–CH_2COOH$ group which represents the

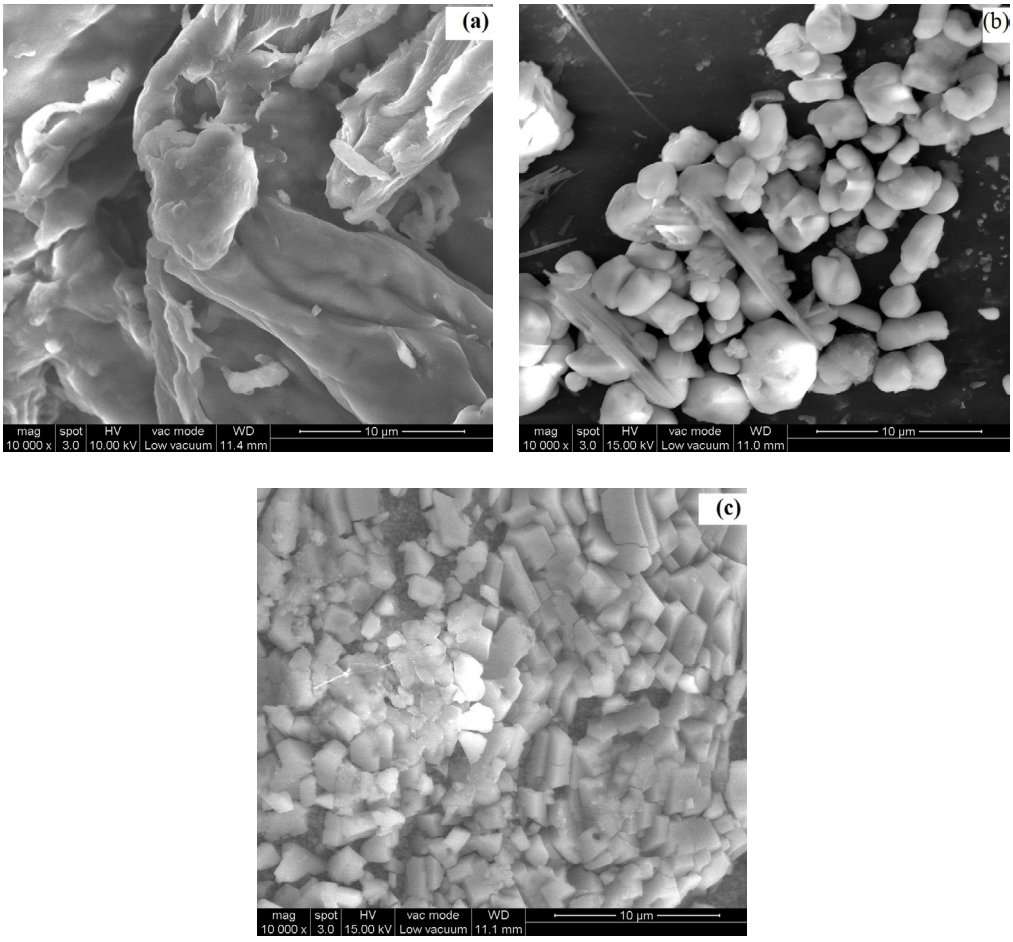

Fig. 2. Scanning electron microscope (SEM) image of (a) CMCh, (b) CMCh-Cs(I) complex, and (c) CMCh-Sr(II) complex.

carboxymethylation on both the amino and hydroxyl groups of chitosan [51,52].

Fig. 4b shows the FTIR spectrum of Cs(I)—CMCh complex. The peak at 2,927 cm^{-1} represents the C–H stretch. The peak at 2,381 cm^{-1} corresponds to C≡C, C≡N stretch. The peak at 1,300 cm^{-1} corresponds to C–C stretch. Fig. 4c shows the FTIR spectrum of Sr(II)-CMCh complex. The peak at 3,378 cm^{-1} corresponds to C–H stretch, which represents the absorbed water with hydrogen bonding. The peak at 1,627 cm^{-1} refers to C≡N stretch, 1,525 cm^{-1} corresponds to N–H stretch and peak at 1,328 cm^{-1} corresponds to C–C stretch.

3.2. Influence of initial pH of the feed solution, P/M, and initial concentration of Sr(II) in feed solution on the percentage rejection of Sr(II)

The 3D response plots representing the interactive effects amongst the process input variables such as initial pH of the feed solution, P/M, and the initial concentration of Sr(II) in feed solution on the percentage rejection of Sr(II) are shown in Fig. 5. It is observed from Fig. 5a that when the initial pH of the feed solution is increased at constant P/M, the percentage rejection of Sr(II) with CMCh increases more rapidly from pH 2 to 12. As the pH increases, the complexation is more favored due to the affinity of carboxyl moiety in CMCh, which dominates the hydroxyl ions in the aqueous solution for binding with the Sr(II). With the increase in the initial pH, percentage rejection of Sr(II) increases [27,53]. As the P/M increases from 0.5 to 2, when the initial pH of the solution is maintained constant, the percentage rejection of Sr(II) drops, and it starts to increase as the P/M increases from 2 to 3. The drop in percentage rejection of Sr(II) is due to the insufficient polymer ligands for complexation with Sr(II). But as the availability of polymer ligands increases, the percentage rejection of Sr(II) also increases and the same is reflected in Fig. 5a from P/M 2 to 3.

The interactive effects among the initial pH of the feed solution and the initial concentration of the feed solution are illustrated in Fig. 5b. The percentage rejection of Sr(II) increases with the initial pH of the feed solution when the initial concentration of feed solution is kept constant. As explained earlier, as the initial pH of the feed solution increases the carboxyl moiety complexes with Sr(II). It is also observed from Fig. 5b that the percentage rejection of Sr(II) increases more significantly with the initial concentration of the feed solution from 2 to 6 mg/L when the initial pH of the solution is maintained constant. The increase in percentage

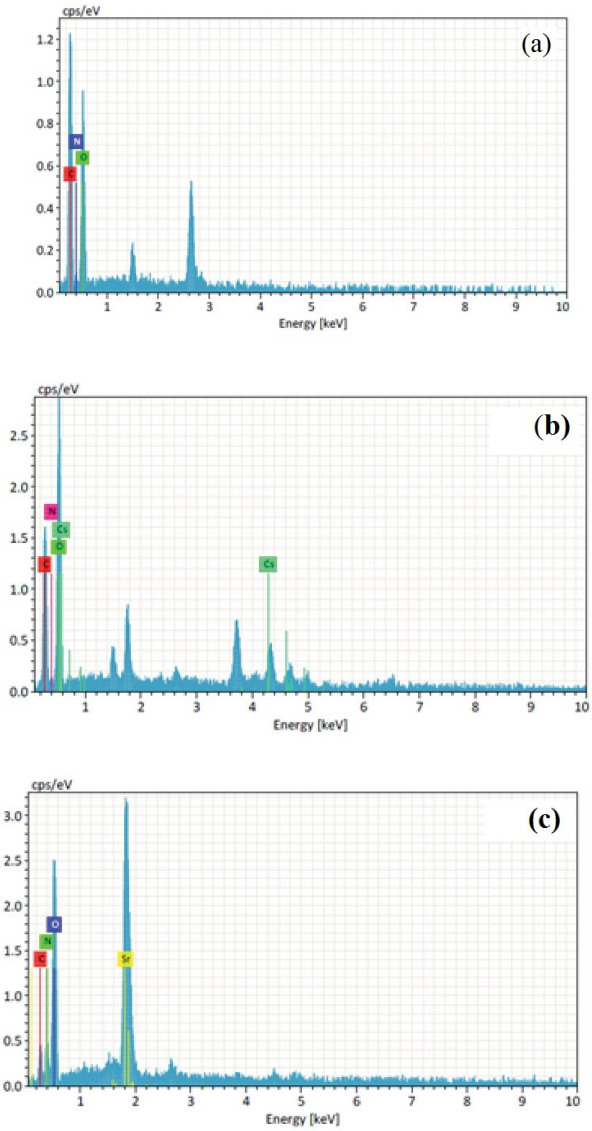

Fig. 3. EDX analysis of (a) CMCh, (b) CMCh-Cs(I) complex, and (c) CMCh-Sr(II) complex.

rejection is because of the presence of more and more Sr(II) for complexation with CMCh. But as the initial concentration of the feed solution increase beyond 8 mg/L, the percentage rejection of Sr(II) drops due to the excess availability of Sr(II) [53].

The interactive effects among P/M and the initial concentration of the feed solution are illustrated in Fig. 5c. It is shown in Fig. 5c that the percentage rejection of Sr(II) decreases as the P/M increases from 0.5 to 2 when the initial concentration of the feed solution is maintained constant. As the availability of polymer ligands are not sufficient for complexation with Sr(II), the percentage rejection of Sr(II) drops. At the same time as the P/M increases from 2 to 3, the percentage rejection of Sr(II) starts to increase due to the presence of sufficient polymer ligands for the complexation with Sr(II). It is also observed from Fig. 5c that the percentage rejection of Sr(II) increases more intensely with an increase in

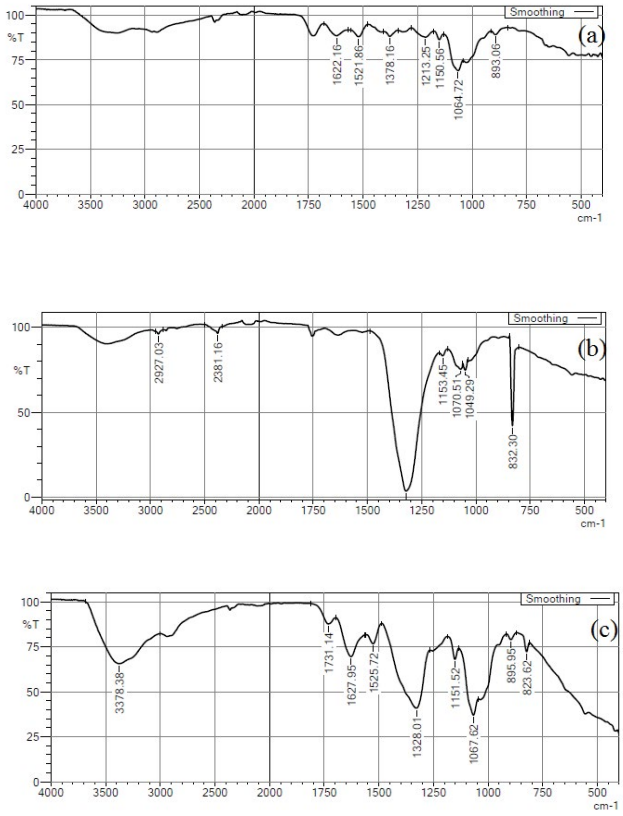

Fig. 4. FTIR spectrum of (a) CMCh, (b) CMCh-Cs(I) complex, (c) CMCh-Sr(II) complex.

the initial concentration of the feed solution from 2 to 8 mg/L, at a constant value of P/M. The rise in the percentage rejection is because of the more availability of the Sr(II) to complex with CMCh. But as the initial concentration of the feed solution increases from 8 to 10 mg/L, the percentage rejection of Sr(II) drops more steeply, since the presence of polymer ligands is excess than its requirement for complexation with Sr(II).

3.3. Influence of initial pH of the feed solution, P/M, and initial concentration of Sr(II) in feed solution on the binding capacity of CMCh with Sr(II)

The response surface 3D plots representing the interactive effects amongst the process input variables on the binding capacity of CMCh with Sr(II) are shown in Fig. 6. It is observed from Fig. 6a that as the initial pH of the feed solution increases at a constant P/M, the binding capacity also increases more rapidly. As mentioned earlier, the increase in the binding capacity is due to the affinity of carboxyl moiety to complex with Sr(II). This behavior remains the same until P/M 1. From P/M 1 to 2 with an increase in the initial pH of the feed solution, the increase in the binding capacity is not significant. The binding capacity drops due to the insufficient ligands for complexation with Sr(II). But beyond P/M 2, the increase in the initial pH of the feed solution does not have any significant effect on the binding capacity of CMCh with Sr(II), since the polymer concentration is quite more than the

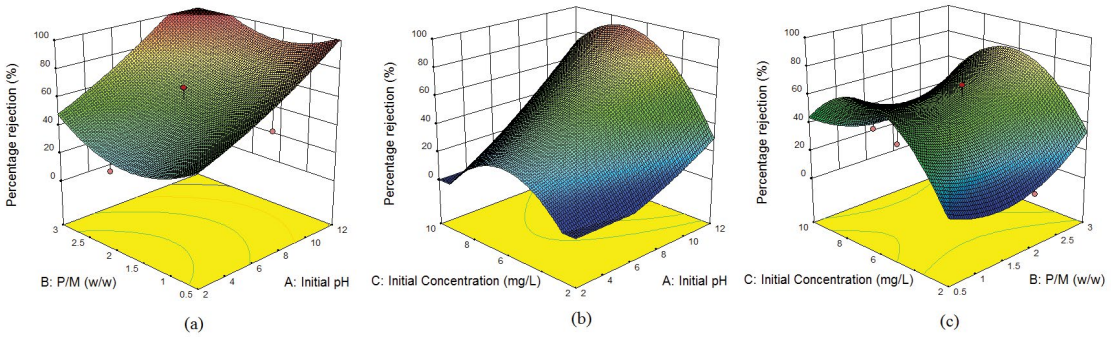

Fig. 5. Percentage rejection of Sr(II) with CMCh (a) interactive effect of initial pH of the feed solution and P/M on percentage rejection, (b) interactive effect of initial pH of the feed solution and initial concentration of Sr(II) on percentage rejection, and (c) interactive effect of P/M and initial concentration of Sr(II) on percentage rejection.

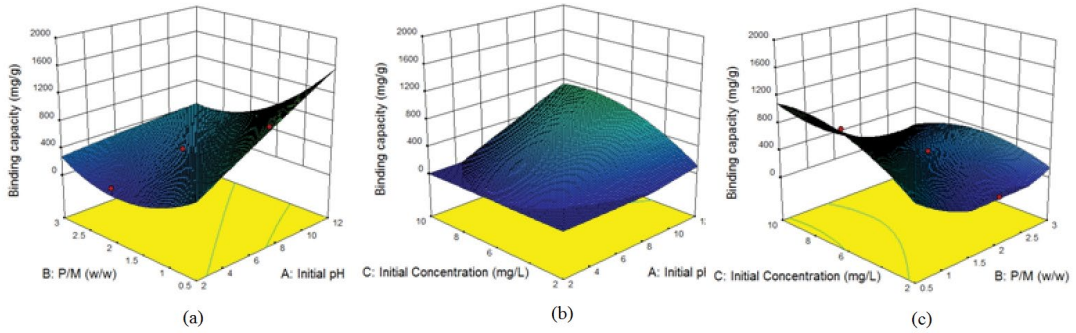

Fig. 6. Binding capacity of CMCh with Sr(II) (a) interactive effect of initial pH of the feed solution and P/M on binding capacity, (b) interactive effect of initial pH of the feed solution and initial concentration of Sr(II) on binding capacity, and (c) interactive effect of P/M and initial concentration of Sr(II) on binding capacity.

requirement for complexation with Sr(II). From Fig. 6a it is also observed that the binding capacity of CMCh with Sr(II) decreases with an increase in P/M from 0.5 to 2 at a constant initial pH of the feed solution. The drop in binding capacity is due to the insufficient ligands for complexation with Sr(II) until P/M 2. Bur further increase in the P/M, increases the binding capacity due to the presence of sufficient ligands for complexation. The above-mentioned behavior is observed from Fig. 6a until the initial pH of the feed solution is 6. Beyond this value, as the P/M increases from 2 to 3, binding capacity of CMCh with Sr(II) nearly remains constant.

It is illustrated in Fig. 6b that as the initial pH of the feed solution increases at a constant initial concentration of Sr(II) in the feed solution, the binding capacity of CMCh with Sr(II) does not change. Although the affinity of carboxyl moiety increases with an increase in the initial pH of the feed solution, because of the insufficient presence of Sr(II), the binding capacity remains constant till the initial concentration 4 mg/L. But beyond this value of the initial concentration of Sr(II) in the feed solution, the binding capacity starts to increase quite significantly as the initial pH of the feed solution increases. The rise in the binding capacity is because of the adequate quantity of Sr(II) for the complexation. It is also observed from Fig. 6b as the initial concentration of Sr(II) increases, the binding capacity of CMCh with Sr(II) remains the same at a constant initial pH of the feed solution. The same behavior is reflected until initial pH 4. As the initial pH of the feed solution is more than four, with an increase in the initial concentration of Sr(II) in feed solution, increases the binding capacity of CMCh with Sr(II), since the quantity of Sr(II) increases.

Fig. 6c reveals that at a constant initial concentration of Sr(II) in the feed solution, the binding capacity of CMCh with Sr(II) drops with rise in P/M value from 0.5 to 1.5, then it remains constant as the P/M value is increased beyond 1.5. The initial drop is due to the inadequate availability of ligands to complex with Sr(II), but beyond P/M 1.5, the constant binding capacity is due to the excessive ligands than its requirement for the complexation with Sr(II). It is also revealed from Fig. 6c, with an increase in the initial concentration of Sr(II) in the feed solution at a constant P/M, the binding capacity of CMCh with Sr(II) increases. However, this behavior is observed in Fig. 6c till the P/M value 1.5. As the initial concentration of Sr(II) increases, the binding capacity remains constant when the P/M value is maintained from 1.5 to 3.

3.4. Influence of initial pH of the feed solution, P/M, and initial concentration of Cs(I) in feed solution on the percentage rejection of Cs(I)

The 3D response surface plots representing the interactive effects amongst the process input variables initial pH of the feed solution, P/M, and the initial concentration of Cs(I)

in the feed solution are represented in Fig. 7. From Fig. 7a it is observed that the percentage rejection of Cs(I) increases gradually with the increase in the initial pH of the feed solution at a constant P/M. The increase in the binding capacity is due to the increase in the affinity of carboxyl moiety in CMCh to complex with Cs(I). It is also revealed from Fig. 7a that, the percentage rejection of Cs(I) does not change with a rise in P/M at a constant initial pH of the feed solution. Since the lower value of P/M itself is sufficient for the complexation because of the adequate quantity of polymer ligands for the complexation and higher the value does not alter the percentage rejection of Cs(I).

With an increase in the initial pH of the feed solution at a constant initial concentration of Cs(I) in the feed solution, the percentage rejection of Cs(I) slightly increases as shown in Fig. 7b. But at the initial concentration of 10 mg/L, there is no perceptible change in the percentage rejection of Cs(I) with the increase in the initial pH of the feed solution. The slight increase in the percentage rejection is due to the affinity of carboxyl moiety in CMCh towards complexation and also due to the adequate quantity of Cs(I) for complexation. Although the affinity of carboxyl moiety is more, the percentage rejection remains constant at the initial concentration of 10 mg/L due to the excessive quantity of Cs(I) than its requirement for the complexation. It is also observed from Fig. 7b, at a constant initial pH of the feed solution, the percentage rejection of Cs(I) increases slightly with an increase in the initial concentration of Cs(I) in the feed solution. But at initial pH value 12, the percentage rejection remains constant with the increase in the initial concentration of Cs(I).

It is revealed from Fig. 7c, at a constant initial concentration of Cs(I) in the feed solution, the percentage rejection of Cs(I) remains nearly constant with the increase in the P/M value, since the P/M and initial concentration are interrelated factors. It is also observed from Fig. 7c that as the initial concentration of Cs(I) in the feed solution increases, the percentage rejection of Cs(I) increases slightly when the P/M value is maintained constant.

3.5. Influence of initial pH of the feed solution, P/M, and initial concentration of Cs(I) in feed solution on the binding capacity of CMCh with Cs(I)

The 3D response surface plots reflecting the interactive effects amongst the process input variables on the process response binding capacity of CMCh with Cs(I)are shown in Fig. 8. It is observed from Fig. 8a that there is no change in the binding capacity of CMCh with Cs(I) with the increase in the initial pH of the feed solution when the P/M value is held constant. However, the affinity of carboxyl moiety in CMCh increases with pH, due to the inadequate availability of CMCh the binding capacity does not change. It is also revealed from Fig. 8a that the binding capacity drops down with the increase in the P/M value till two when the initial pH of the feed solution is kept constant. The drop in binding capacity of CMCh with Cs(I) is due to the insufficient

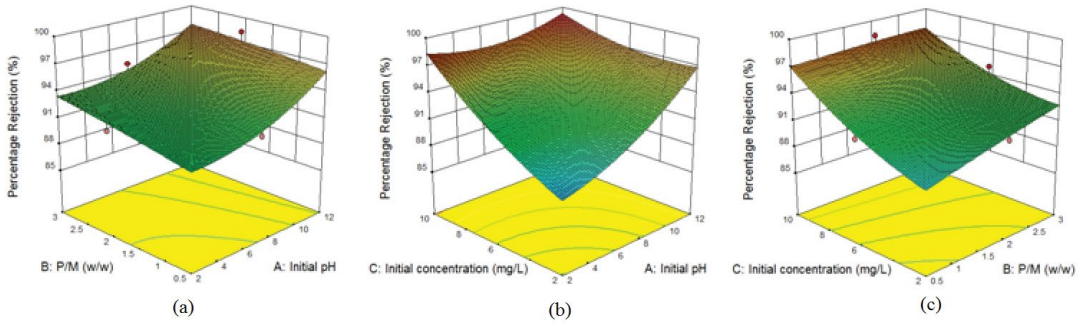

Fig. 7. Percentage rejection of Cs(I) with CMCh (a) interactive effect of initial pH of the feed solution and P/M on percentage rejection, (b) interactive effect of initial pH of the feed solution and initial concentration of Cs(I) on percentage rejection, and (c) interactive effect of P/M and initial concentration of Cs(I) on percentage rejection.

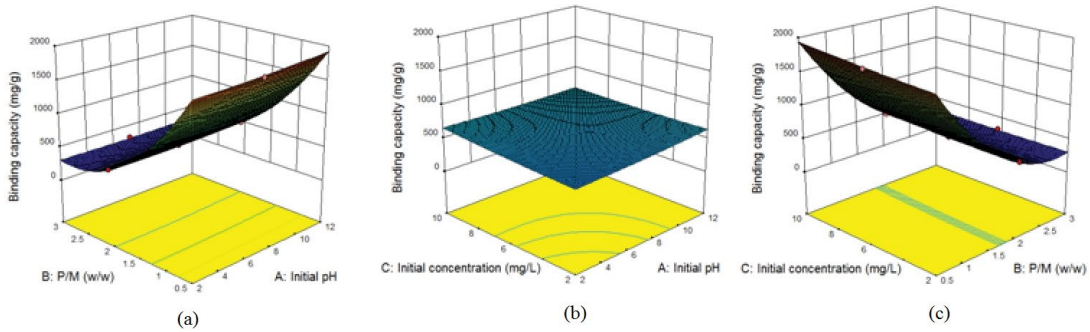

Fig. 8. Binding capacity of CMCh with Cs(I) (a) interactive effect of initial pH of the feed solution and P/M on binding capacity, (b) interactive effect of initial pH of the feed solution and initial concentration of Cs(I) on binding capacity, and (c) interactive effect of P/M and initial concentration of Cs(I) on binding capacity.

quantity of polymer ligands for complexation with Cs(I). When the P/M value is increased further, the binding capacity remains constant. The binding capacity remains constant because of the excessive quantity of polymer ligands than its requirement for complexation.

From Fig. 8b it is observed that the interactive effects of initial pH of the feed solution and the initial concentration of Cs(I) in the feed solution do not have a significant influence on the binding capacity of CMCh with Cs(I).

It is reflected in Fig. 8c, as the P/M value increases from 0.5 to 2, the binding capacity drops perceptively when the initial concentration of Cs(I) in the feed solution is maintained constant. But with further increase in the P/M value, the binding capacity of CMCh with Cs(I) remains constant. Since the availability of polymer ligands for the complexation is not sufficient until P/M value 2, beyond this, the polymer ligands become excess than its requirement for complexation. It is also shown in Fig. 8c that the increase in the initial concentration does not reflect any change in the binding capacity of CMCh with Cs(I).

3.6. Analysis of variance

To ensure the fitness of a model and the significance of individual model coefficients, ANOVA was performed. The ANOVA table for the process response percentage rejection of Sr(II) and the binding capacity of CMCh with Sr(II) are shown in Tables 3, 4, respectively. The process input variables initial pH of the feed solution, and initial concentration of Sr(II) have a significant effect on the process response percentage rejection of Sr(II) as the *P*-value is <0.05. But the P/M has no significant effect on the percentage rejection of Sr(II) as its *P*-value is more than 0.05. Concerning the interactive effects amongst these process input variables on the process

Table 3
ANOVA table for the percentage rejection of Sr(II) using CMCh

Source	Sum of squares	*df*	Mean square	*F* value	*p*-value Prob > *F*	
Model	17,731.11	9	1,970.12	10.313	0.000553898	Significant
A-initial pH	10,309.49	1	10,309.49	53.967	2.46461E-05	
B-P/M	308.136	1	308.14	1.613	0.2328	
C-initial concentration	1,113.463	1	1,113.46	5.829	0.0364	
AB	83.56133	1	83.56	0.437	0.5233	
AC	921.4925	1	921.49	4.824	0.0528	
BC	219.1835	1	219.18	1.147	0.3093	
A^2	60.54791	1	60.55	0.317	0.5858	
B^2	940.2771	1	940.28	4.922	0.0508	
C^2	4,321.751	1	4,321.75	22.623	0.0007728	
Residual	1,910.35	10	191.035			
Lack of fit	1,910.35	5	382.07			
Pure error	0	5	0			
Cor. Total	19,641.46	19				

Table 4
ANOVA table for the binding capacity of CMCh with Sr(II)

Source	Sum of Squares	*df*	Mean square	*F* value	*p*-value Prob > *F*	
Model	3,633,923	9	4,03,769.3	15.001	0.000108	Significant
A-initial pH	1,071,491	1	1,071,491	39.809	8.8E-05	
B-P/M	1,000,014	1	1,000,014	37.153	0.000116	
C-initial concentration	2,53,314.1	1	2,53,314.1	9.411	0.011886	
AB	4,93,230.2	1	4,93,230.2	18.325	0.00161	
AC	1,90,303.4	1	1,90,303.4	7.070	0.023941	
BC	2,32,109.4	1	2,32,109.4	8.623	0.014873	
A^2	502.0316	1	502.0316	0.01865	0.89408	
B^2	2,90,975.7	1	2,90,975.7	10.810	0.008179	
C^2	1,52,109.7	1	1,52,109.7	5.651	0.038795	
Residual	2,69,160.9	10	26,916.09			
Lack of fit	2,69,160.9	5	53,832.19			
Pure error	0	5	0			
Cor. total	3,903,084	19				

response percentage rejection of Sr(II), does not have any significant impact as their *P*-value is more than 0.05. The *R*-squared value for the percentage rejection of Sr(II) is 0.91, which is nearly close to 1 and acceptable. It implies that 91% of the variability in the data is explained by the predicted model.

The process input variables initial pH of the feed solution, P/M, and initial concentration of Sr(II) in the feed solution have a significant effect on the process response binding capacity of CMCh with Sr(II) as the *P*-value is <0.05. The interactive effects amongst these process input variables are also significant as their *P*-value is <0.05. The R^2 value for the binding capacity of CMCh with Sr(II) is 0.93, close to 1.0, which is acceptable. The value of R^2 implies that 93% of the variability in the data can be explained by the predicted model.

The ANOVA table for the process response percentage rejection of Cs(I) and the binding capacity of CMCh with Cs(I) are shown in Tables 5, 6, respectively. The interactive effects of the initial pH of the feed solution and the initial concentration of Cs(I) in the feed solution on the process response percentage rejection of Cs(I) are significant since the *P*-value is <0.05. The R^2 value for the percentage rejection of Cs(I) is 0.97, close to 1.0, which is acceptable. The R^2 value reflects that 97% of the variability in the data can be explained by the predicted model. The individual effects and interactive effects of process input variables have a significant effect on the process response binding capacity of CMCh with Cs(I) since the *P*-value is <0.05. The R^2 value for the binding capacity of CMCh with Cs(I) is 0.99, very close to 1.0, which is acceptable. Also, it shows that 99% of the variance in the data can be explained by the predicted model.

The normal probability plot of the internally studentized residuals is shown in Figs. 9 and 10. All the points on these plots lie either on the straight line or reasonably close to the

Table 5
ANOVA table for the percentage rejection of Cs(I) using CMCh

Source	Sum of squares	*df*	Mean square	*F* value	*p*-value Prob > *F*	
Model	227.853	9	25.317	42.227	8.7787E–07	significant
A-initial pH	61.055	1	61.055	101.834	1.4624E–06	
B-P/M	12.056	1	12.056	20.108	0.001171	
C-initial concentration	103.372	1	103.372	172.415	1.2473E–07	
AB	0.7716	1	0.7716	1.287	0.2831	
AC	31.601	1	31.601	52.708	2.7261E–05	
BC	4.637	1	4.637	7.735	0.01941	
A^2	4.848	1	4.848	8.086	0.01744	
B^2	0.0376	1	0.0376	0.06282	0.8072	
C^2	2.392	1	2.392	3.990	0.07368	
Residual	5.996	10	0.5996			
Lack of fit	5.996	5	1.199			
Pure error	0	5	0			
Cor. total	233.849	19				

Table 6
ANOVA table for the binding capacity of CMCh with Cs(I)

Source	Sum of squares	*df*	Mean square	*F* value	*p*-value Prob > *F*	
Model	8,092,303.7	9	8,99,144.9	1,549.003	1.61E–14	significant
A-initial pH	7,557.43	1	7,557.439	13.019	0.004782	
B-P/M	6,068,519.1	1	6,068,519	10,454.55	1.96E–16	
C-initial concentration	15,175.99	1	15,175.99	26.144	0.000455	
AB	4,294.24	1	4,294.239	7.398	0.02156	
AC	5,886.13	1	5,886.125	10.140	0.009747	
BC	10,148.35	1	10,148.35	17.483	0.001884	
A^2	559.242	1	559.2416	0.963	0.3495	
B^2	5,69,750.4	1	5,69,750.4	981.538	2.58E-11	
C^2	415.064	1	415.0641	0.715	0.4175	
Residual	5,804.67	10	580.4668			
Lack of fit	5,804.67	5	1,160.934			
Pure error	0	5	0			
Cor. total	8,098,108.4	19				

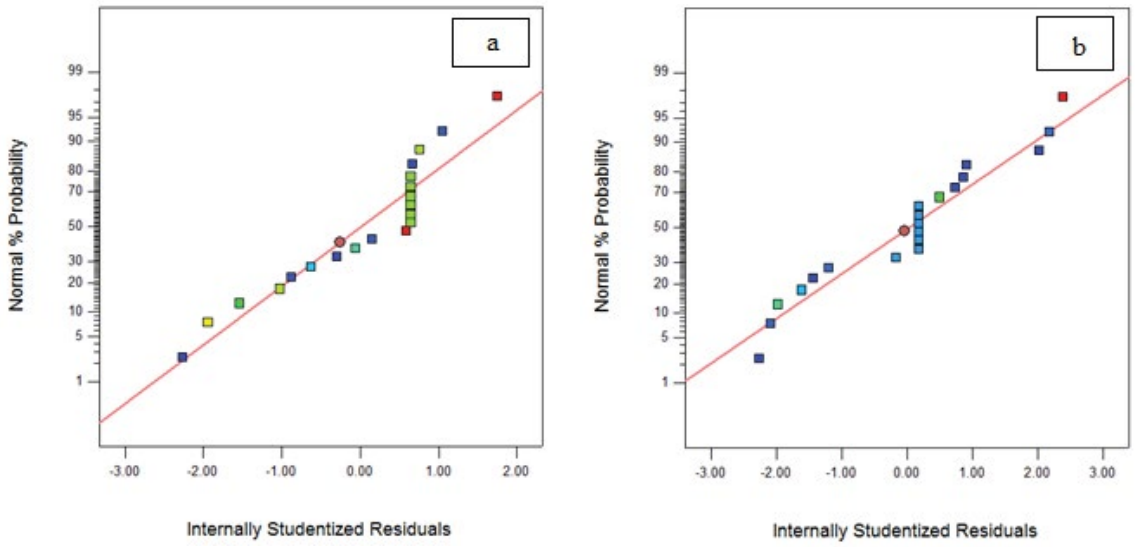

Fig. 9. Normal plot of residuals (a) percentage rejection of Sr(II) with CMCh and (b) binding capacity of CMCh with Sr(II).

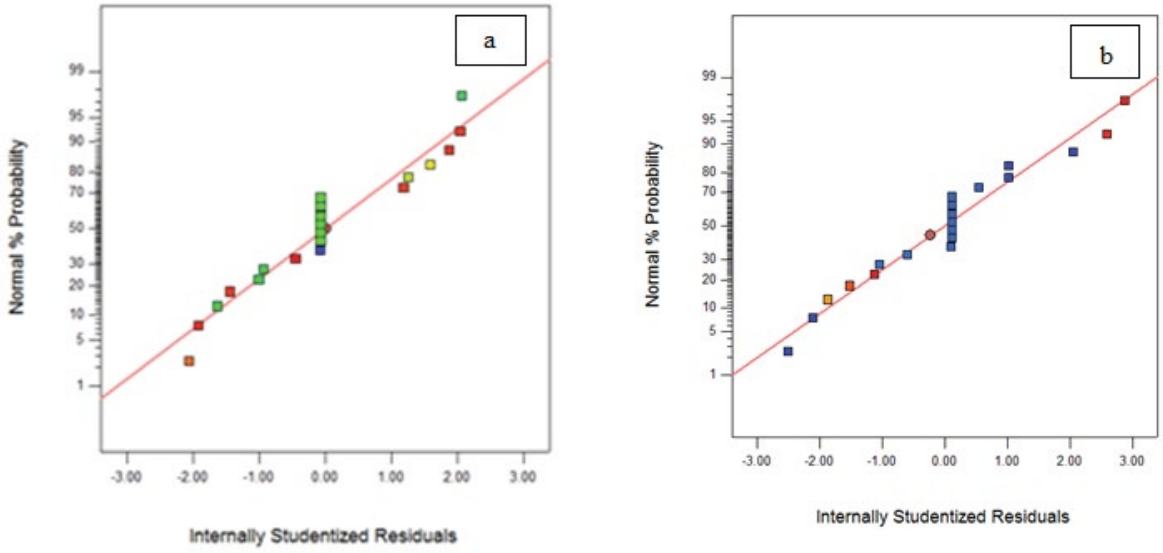

Fig. 10. Normal plots of residuals (a) percentage rejection of Cs(I) with CMCh and (b) binding capacity of CMCh with Cs(I).

straight line. This confirms that the errors were normally distributed. This can be taken as an additional tool to verify the competency of the final model.

3.7. Empirical model equations for the percentage rejection of Sr(II)

The empirical model equation for the percentage rejection of Sr(II), R expressed in terms of the coded and actual variables are given by the following Eqs. (7) and (8):

$$R = 54.3122 + 32.1402 \times A + 5.551 \times B + 10.5625 \times C + 3.21905 \times AB + 10.7325 \times AC - 5.21349 \times BC + 4.69227 \times A^2 + 19.3672 \times B^2 - 39.6427 \times C^2 \quad (7)$$

$$R = -38.4397 - 0.320708 \times \text{Initial pH} - 36.2908 \times \text{P/M} + 30.441 \times \text{Initial Concentration} + 0.515048 \times \text{Initial pH} \times \text{P/M} + 0.536625 \times \text{Initial pH} \times \text{Initial Concentration} - 1.0427 \times \text{P/M} \times \text{Initial Concentration} + 0.187691 \times \text{Initial pH}^2 + 12.395 \times \text{P/M}^2 - 2.47767 \times \text{Initial Concentration}^2 \quad (8)$$

3.8. Empirical model equations for the binding capacity of CMCh with Sr(II)

The empirical model equation for the Binding capacity of CMCh with Sr(II), q expressed in terms of the coded and actual variables are given by the following Eqs. (9) and (10):

$$q = 345.393 + 327.661 \times A - 316.23 \times B + 159.316 \times C - 247.314 \times \mathrm{AB} + 154.233 \times \mathrm{AC} - 169.657 \times \mathrm{BC} - 13.5114 \times A^2 + 340.695 \times B^2 - 235.186 \times C^2 \quad (9)$$

$$q = -314.599 + 96.0766 \times \text{Initial pH} - 535.562 \times \text{P/M} + 221.617 \times \text{Initial Concentration} - 39.5703 \times \text{Initial pH} \times \text{P/M} + 7.71167 \times \text{Initial pH} \times \text{Initial Concentration} - 33.9313 \times \text{P/M} \times \text{Initial Concentration} - 0.540455 \times \text{Initial pH}^2 + 218.045 \times \text{P/M}^2 - 14.6991 \times \text{Initial Concentration}^2 \quad (10)$$

3.9. Empirical model equations for the percentage rejection of Cs(I)

The empirical model equation for the percentage rejection of Cs(I), R expressed in terms of the coded and actual variables are given by the following Eqs. (11) and (12):

$$R = 93.3322 + 2.47337 \times A + 1.098 \times B + 3.21833 \times C - 0.309325 \times AB - 1.9875 \times AC - 0.758333 \times BC + 1.32773 \times A^2 - 0.122576 \times B^2 + 0.93272 \times C^2 \quad (11)$$

$$R = 81.593 + 0.434008 \times \text{Initial pH} + 2.40941 \times \text{P/M} + 1.06608 \times \text{Initial concentration} - 0.0494921 \times \text{Initial pH} \times \text{P/M} - 0.099375 \times \text{Initial pH} \times \text{Initial concentration} - 0.151667 \times \text{P/M} \times \text{Initial concentration} + 0.0531091 \times \text{Initial pH}^2 + - 0.0784485 \times \text{P/M}^2 + 0.0582955 \times \text{Initial concentration}^2 \quad (12)$$

3.10. Empirical model equations for the binding capacity of CMCh with Cs(I)

The empirical model equation for the binding capacity of CMCh with Cs(I), q expressed in terms of the coded and actual variables are given by the following Eqs. (13) and (14):

$$q = 601.418 + 27.5181 \times A - 779.007 \times B + 38.995 \times C - 23.0764 \times AB - 27.125 \times AC - 35.475 \times BC + 14.2605 \times A^2 + 476.739 \times B^2 + 12.2855 \times C^2 \quad (13)$$

$$q = 2408.32 + 12.1166 \times \text{Initial pH} - 1622.68 \times \text{P/M} + 22.4447 \times \text{Initial concentration} - 3.69222 \times \text{Initial pH} \times \text{P/M} - 1.35625 \times \text{Initial pH} \times \text{Initial concentration} - 7.095 \times \text{P/M} \times \text{Initial concentration} + 0.570418 \times \text{Initial pH}^2 + 305.113 \times \text{P/M}^2 + 0.767841 \times \text{Initial concentration}^2 \quad (14)$$

The empirical equations for the percentage rejection of Sr(II) and Cs(I) expressed in terms of coded factors are used to make predictions about the response percentage rejection for given levels of each factor. The high levels of the factors are codes as +1, and the low levels of the factors are coded as –1. This equation is used to identify the relative influence of the factors by comparing the factor coefficients.

The empirical equations for the percentage rejection of Sr(II) and Cs(I) expressed in terms of the actual factors can be used to make predictions about the response binding capacity for the given levels of each factor. Here, the levels should be specified in the original units for each factor. These equations cannot be used to determine the relative influence of each factor because the coefficients are scaled to accommodate the units of each factor.

3.11. Optimization of process input variables

The process input variables initial pH of the feed solution, P/M, and the initial concentration of Sr(II) and Cs(I) in the feed solution were optimized to maximize the process responses percentage rejection of Sr(II) and Cs(I) and the binding capacity of CMCh with Sr(II) and Cs(I). The maximum percentage rejection, 99.6% of Sr(II) with CMCh, and the maximum binding capacity, 1,800 mg/g of CMCh with Sr(II) were found to be obtained at the following optimum values: The initial pH of the feed solution is 12, P/M value is 0.5, and the initial concentration is 9 mg/L.

The maximum percentage rejection, 99.14% of Cs(I) with CMCh and the maximum binding capacity 1,982 mg/g of CMCh with Cs(I) were found to be obtained at the following optimum values: The initial pH of the feed solution is 12, P/M value is 0.5, and the initial concentration is 10 mg/L. However, more than 97% rejection of Cs(I) with a binding capacity of 1,950 mg/g was obtained in the pH range of 7–8. So, the maximum recovery can be achieved without much altering the initial pH of the feed solution, which intern reduces the volume of sludge and requirement of chemicals for the adjustment of pH of the feed solution.

4. Conclusions

This present study investigated the (i) success of SEUF for the removal of Sr(II) and Cs(I), (ii) competence of CMCh as a size enhancing agent, and (iii) the DoE by RSM. The experimental findings, percentage rejection and binding capacity of CMCh show that SEUF process is a promising method for the removal of Sr(II) and Cs(I). It has also been proved that CMCh could be an excellent size enhancing species for getting the removal of Sr(II) and Cs(I) from aqueous streams. The maximum percentage rejection of 99% of Sr(II) and Cs(I) was obtained at the optimum values. The optimum values for the maximum percentage rejection of Sr(II) are as follows: Initial pH of the feed solution is 12, P/M value is 0.5, and initial concentration of Sr(II) in the feed solution is 9 mg/L. The optimum values for the maximum percentage rejection of Cs(I) are as follows: Initial pH of the feed solution is 12, P/M value is 0.5 and initial concentration of Cs(I) in the feed solution is 10 mg/L. However, It is also observed from the results that about 97% rejection of Cs(I) can be possible without much altering the initial pH of the feed solution. It has also been proved that the RSM as an efficient mathematical and statistical tool, which took into account all the essential aspects of the process to achieve the maximum percentage rejection and binding capacity. ANOVA indicated the significance of the predicted model and the individual process input variables and the interactive effects amongst those variables on the percentage rejection and the binding capacity.

The optimum values of the process variables were obtained for maximizing the process responses. The optimum values were verified with the experimentally found values to check the consistency. The quadratic equations developed for the percentage rejection and the binding capacity show the presence of a high correlation between observed and predicted values.

Acknowledgments

The authors would like to thank Nanotechnology Research center, SRMIST, Kattankulathur, Tamil Nadu, India and SAIF, IIT Madras, Chennai, Tamil Nadu, India for the SEM, EDX, and FTIR analysis.

References

[1] M.A.H. Bhuiyan, M.A. Islam, S.B. Dampare, L. Parvez, S.Suzuki, Evaluation of hazardous metal pollution in irrigation and drinking water systems in the vicinity of a coal mine area of northwestern Bangladesh, J. Hazard. Mater., 179 (2010) 1065–1077.
[2] Q.A. Malik, M.S. Khan, Effect on human health due to drinking water contaminated with heavy metals, J. Pollut. Eff. Control, 5 (2016) 1000179.
[3] A.E. Burakov, E.V. Galunin, I.V. Burakova, A.E. Kucherova, S. Agarwal, A.G. Tkachev, V.K. Gupta, Adsorption of heavy metals on conventional and nanostructured materials for wastewater treatment purposes: a review, Ecotoxicol. Environ. Saf., 148 (2018) 702–712.
[4] E.D. Hwang, K.W. Lee, K.H. Choo, S.J. Choi, S.H. Kim, C.H. Yoon, C.H. Lee, Effect of precipitation and complexation on nanofiltration of strontium-containing nuclear wastewater, Desalination, 147 (2002) 289–294.
[5] J. Peterson, M. MacDonell, L. Haroun, F. Monette, Radiological and Chemical Fact Sheets to Support Health Risk Analyses for Contaminated Areas, U.S. Department of Energy, United States, 2007.
[6] A. Nilchi, M.R. Hadjmohammadi, S.R. Garmarodi, R. Saberi, Studies on the adsorption behavior of trace amounts of $90Sr^{2+}$, $140La^{3+}$, $60Co^{2+}$, Ni^{2+} and Zr^{4+} cations on synthesized inorganic ion exchangers, J. Hazard. Mater., 167 (2009) 531–535.
[7] L. Wu, G. Zhang, Q. Wang, L. Hou, P. Gu, Removal of strontium from liquid waste using a hydraulic pellet co-precipitation microfiltration (HPC-MF) process, Desalination, 349 (2014) 31–38.
[8] T. Sangvanich, V. Sukwarotwat, R.J. Wiacek, R.M. Grudzien, G.E. Fryxell, R.S. Addleman, C. Timchalk, W. Yantasee, Selective capture of cesium and thallium from natural waters and simulated wastes with copper ferrocyanide functionalized mesoporous silica, J. Hazard. Mater., 182 (2010) 225–231.
[9] G. Gurboga, H. Tel, Preparation of TiO_2–SiO_2 mixed gel spheres for strontium adsorption, J. Hazard. Mater., 120 (2005) 135–142.
[10] E.I. Kurbatova, A.I. Ksenofontov, A.M. Dmitriyev, J.L. Regens, Irradiation of sorbents by ions of polymorphic metals for modeling 90 strontium sedimentation, Environ. Sci. Pollut. Res., 14 (2007) 251–255.
[11] A. Ahmadpour, M. Zabihi, M. Tahmasbi, T.R. Bastami, Effect of adsorbents and chemical treatments on the removal of strontium from aqueous solutions, J. Hazard. Mater., 182 (2010) 552–556.
[12] A. Ghaemi, M. Torab Mostaedi, M. Ghannadi Maragheh, Characterizations of strontium(II) and barium(II) adsorption from aqueous solutions using dolomite powder, J. Hazard. Mater., 190 (2011) 916–921.
[13] M. Cabranes, A.G. Leyva, P.A. Babay, Removal of Cs^+ from aqueous solutions by perlite, Environ. Sci. Pollut. Res., 25 (2018) 21982–21992.
[14] J.L. Parks, M. Edwards, Precipitative removal of As, Ba, B, Cr, Sr, and V using sodium Carbonate, J. Environ. Eng., 132 (2006) 489–496.
[15] V. Pacary, Y. Barre, E. Plasari, Method for the prediction of nuclear waste solution decontamination by co-precipitation of strontium ions with barium sulphate using the experimental data obtained in non-radioactive environment, Chem. Eng. Res. Des., 88 (2010) 1142–1147.
[16] S. Tan, X. Chen, Y. Ye, J. Sun, L. Dai, Q. Ding, Hydrothermal removal of Sr^{2+} in aqueous solution via formation of Sr-substituted hydroxyapatite, J. Hazard. Mater., 179 (2010) 559–563.
[17] R.W. Warrant, J.G. Reynolds, M. Johnson, Removal of ^{90}Sr and ^{241}Am from concentrated Hanford chelate-bearing waste by precipitation with strontium nitrate and sodium permanganate, J. Radioanal. Nucl. Chem., 295 (2013) 1575–1579.
[18] A.J. Rabideau, J.V. Benschoten, A. Patel, K. Bandilla, Performance assessment of a zeolite treatment wall for removing Sr-90 from groundwater, J. Contam. Hydrol., 79 (2005) 1–24.
[19] B. Ma, S. Oh, W.S. Shin, S. Choi, Removal of Co^{2+}, Sr^{2+} and Cs^+ from aqueous solution by phosphate-modified montmorillonite (PMM), Desalination, 276 (2011) 336–346.
[20] W. Guan, J. Pan, H. Ou, X. Wang, X. Zou, W. Hu, C. Li, X. Wu, Removal of strontium(II) ions by potassium tetratitanate whisker and sodium trititanate whisker from aqueous solution: equilibrium, kinetics and thermodynamics, Chem. Eng. J., 167 (2011) 215–222.
[21] R. Dabbagh, H. Ghafourian, A. Baghvand, G.R. Nabi, H. Riahi, M.A.A. Faghih, Bioaccumulation and biosorption of stable strontium and ^{90}Sr by *Oscillatoria homogenea* cyanobacterium, J. Radioanal. Nucl. Chem., 272 (2007) 53–59.
[22] S.G. Mashkani, P.T.M. Ghazvini, Biotechnological potential of Azolla filiculoides for biosorption of Cs and Sr: application of micro-PIXE for measurement of biosorption, Bioresour. Technol., 100 (2009) 1915–1921.
[23] N. Ngwenya, E.M.N. Chirwa, Single and binary component sorption of the fission products Sr^{2+}, Cs^+ and Co^{2+} from aqueous solutions onto sulphate reducing bacteria, Miner. Eng., 23 (2010) 463–470.
[24] L.H.V. Thanh, J.C. Liu, Flotation separation of strontium via phosphate precipitation, Water Sci. Technol., 75 (2017) 2520–2526.
[25] T. Vincent, C. Vincent, E. Guibal, Immobilization of metal hexacyanoferrate ion-exchangers for the synthesis of metal ion sorbents—a mini-review, Molecules, 20 (2015) 20582–20613.
[26] P.K. Sinha, R.V. Amalraj, V. Krishnasamy, Flocculation studies on freshly precipitated copper ferrocyanide for the removal of caesium from radioactive liquid waste, Waste Manage., 13 (1993) 341–350.
[27] S. Divakarana, D. Ponrajua, S. Varugheseb, T. Swaminathan, Parametric studies for strontium separation and volume reduction of a simulated nuclear waste solution, Sep. Sci. Technol., 53 (2018) 1732–1740.
[28] X. Zhang, P. Gu, Y. Liu, Decontamination of radioactive wastewater: state of the art and challenges forward, Chemosphere, 215 (2019) 543–553.
[29] S.V.S. Rao, B. Paul, K.B. Lal, S.V. Narasimhan, J. Ahmed, Effective removal of cesium and strontium from radioactive wastes using chemical treatment followed by ultra filtration, J. Radioanal. Nucl. Chem., 246 (2000) 413–418.
[30] S. Lin, T. Wang, R. Juang, Metal rejection by nanofiltration from diluted solutions in the presence of complexing agents, Sep. Sci. Technol., 39 (2004) 363–376.
[31] L.A. Richards, B.S. Richards, A.I. Schafer, Renewable energy powered membrane technology: salt and inorganic contaminant removal by nanofiltration/reverse osmosis, J. Membr. Sci., 369 (2011) 188–195.
[32] E. Kavitha, M.P. Rajesh, S. Prabhakar, A. Sowmya, M.A. Raqeeb, S. Sriram, P. Jain, Size enhanced ultrafiltration – a novel hybrid membrane process for the removal and recovery of heavy metal contaminants, Res. J. Pharm. Biol. Chem. Sci., 8 (2017) 191–200.
[33] C.A. Rodrigues, M.C.M. Laranjeira, V.T. De Favere, E. Stadler, Interaction of Cu(II) on N-(2-pyridylmethyl) and N-(4-pyridylmethyl) chitosan, Polymer, 39 (1998) 5121–5126.
[34] T. Becker, M. Schlaak, H. Strasdeit, Adsorption of nickel (II), zinc (II) and cadmium (II) by new chitosan derivatives, React. Funct. Polym., 44 (2000) 289–298.

[35] T. Asakawa, K. Inoue, T. Katsutoshi, T. Tanaka, Adsorption of silver on dithiocarbamate type of chemically modified chitosan, Kagaku Kogaku Ronbun., 26 (2000) 321–326, doi: 10.1252/kakoronbunshu.26.321.
[36] Z. Yang, Y. Wang, Y. Tang, Synthesis and adsorption properties for metal ions of mesocyclic diamine-grafted chitosan-crown ether, J. Appl. Polym. Sci., 75 (2000) 1255–1260.
[37] A. Bernkop Schnurch, C. Paikl, C. Valenta, Novel bioadhesive chitosan-EDTA conjugate protects leucine enkephalin from degradation by aminopeptidase N, Pharmacol. Res., 14 (1997) 917–922.
[38] B. Li, F. Zhou, K. Huang, Y. Wang, S. Mei, Y. Zhou, T. Jing, Environmentally friendly chitosan/PEI-grafted magnetic gelatin for the highly effective removal of heavy metals from drinking water, Sci. Rep., 7 (2017) 43082.
[39] F.G.L. Medeiros Borsagli, A.A.P. Mansur, P. Chagas, L.C.A. Oliveira, H.S. Mansur, O-carboxymethyl functionalization of chitosan: complexation and adsorption of Cd(II) and Cr(VI) as heavy metal pollutant ions, React. Funct. Polym., 97 (2015) 37–47.
[40] E. Kavitha, A. Sowmya, S. Prabhakar, P. Jain, R. Surya, M.P. Rajesh, Removal and recovery of heavy metals through size enhanced ultrafiltration using chitosan derivatives and optimization with response surface modeling, Int. J. Biol. Macromol., 132 (2019) 278–288.
[41] M.J. Anderson, P.J. Whitcomb, RSM Simplified: Optimizing Processes Using Response Surface Methods for Design of Experiments, 2nd ed., CRC Press, A Productivity Press Book, Taylor & Francis Group, United States, 2016.
[42] M. Savasari, M. Emadi, M.A. Bahmanyar, P. Biparva, Optimization of Cd(II) removal from aqueous solution by ascorbic acid-stabilized zero valent iron nanoparticles using response surface methodology, J. Ind. Eng. Chem., 21 (2015) 1403–1409.
[43] A. Ahmadia, S. Heidarzadeh, A.R. Mokhtari, E. Darezereshki, H. Asadi Harouni, Optimization of heavy metal removal from aqueous solutions by maghemite (γ-Fe_2O_3) nanoparticles using response surface methodology, J. Geochem. Explor., 147 (2014) 151–158.
[44] N. Maximous, G. Nakhla, W. Wan, K. Wong, Preparation, characterization and performance of Al_2O_3/PES membrane for wastewater filtration, J. Membr. Sci., 341 (2009) 67–75.
[45] S. Velu, L. Muruganandam, G. Arthanareeswaran, Preparation and performance studies on polyethersulfone ultrafiltration membranes modified with gelatin for treatment of tannery and distillery wastewater, Braz. J. Chem. Eng., 32 (2015) 179–189.
[46] C. Cojocaru, G. Zakrzewska-Trznadel, Response surface modeling and optimization of copper removal from aqua solutions using polymer assisted ultrafiltration, J. Membr. Sci., 298 (2007) 56–70.
[47] S. Chakraborty, J. Dasgupta, U. Farooq, J. Sikder, E. Drioli, S. Curcio, Experimental analysis, modeling and optimization of chromium(VI) removal from aqueous solutions by polymer-enhanced ultrafiltration, J. Membr. Sci., 456 (2014) 139–154.
[48] J.L. Aguirre, E. Pongracz, P. Peramaki, R.L. Keiski, Micellar-enhanced ultrafiltration for the removal of cadmium and zinc: use of response surface methodology to improve understanding of process performance and optimization, J. Hazard. Mater., 180 (2010) 524–534.
[49] C. Cojocaru, G. Zakrzewska Trznadel, A. Jaworska, Removal of cobalt ions from aqueous solutions by polymer assisted ultrafiltration using experimental design approach. Part 1: optimization of complexation conditions, J. Hazard. Mater., 169 (2009) 599–609.
[50] A. Koehring, The Application of Polynomial Response Surface and Polynomial Chaos Expansion Meta models within an Augmented Reality Conceptual Design Environment, Dissertation, Iowa State University, Ames, Iowa, 2008.
[51] V.K. Mourya, N.N. Inamdar, A. Tiwari, Carboxymethyl chitosan and its applications, Adv. Mater. Lett., 1 (2010) 11–33.
[52] R.K. Farag, R.R. Mohamed, Synthesis and characterization of carboxymethyl chitosan nanogels for swelling studies and antimicrobial activity, Molecules, 18 (2013) 190–203.
[53] L. Chen, X. Bian, X. Lu, Removal of strontium from simulated low-level radioactive wastewater by nanofiltration, Water Sci. Technol., 78 (2018) 1733–1740.